Elastic scattering of positrons and electrons by argon

Sultana N. Nahar and J. M. Wadehra
Department of Physics and Astronomy, Wayne State University, Detroit, Michigan 48202
(Received 15 September 1986)

Differential and integrated cross sections for the elastic scattering of low- and intermediate-energy (3—300 eV) positrons and electrons by argon atoms are calculated. Higher transport cross sections, representing moments of $1-(\cos\theta)^n$, for these systems are also obtained for $n=1$—4. Model potentials are used to represent the interactions between positrons or electrons and argon atoms. For each impact energy, the phase shifts of the lower partial waves are obtained exactly by numerical integration of the radial equation. The Born approximation is used to obtain the contribution of the higher partial waves to the scattering amplitude. The phase shifts of the seven lowest partial waves are tabulated for various impact energies of positrons and electrons.

I. INTRODUCTION

Since the pioneer work of Ramsauer,[1] the study of electron scattering by noble gases has been of considerable theoretical and experimental interest. Observations and calculations of both the total collisional as well as elastic differential and integrated cross sections for the scattering of electrons by rare-gas atoms have been made. In particular, low-energy total collisional cross sections, for electron scattering, exhibit a Ramsauer-Townsend (RT) minimum for Ar, Kr, and Xe. Observations of the scattering of positrons by rare-gas atoms are relatively recent. "First generation experiments" on positron scattering included observations of the total collisional cross sections.[2] It was then observed that the scattering of positrons by only the lighter rare-gas atoms He, Ne, and possibly Ar, exhibited the RT minimum. Thus argon may play a unique role in exhibiting the RT minimum for the scattering of both the electrons and the positrons. With the advent of high-intensity positron beams, it has now become feasible to carry out "second generation experiments" for measurements of angular distribution of positrons elastically scattered by rare-gas atoms. The impetus for the present paper is provided by the recent measurement[3] of differential cross sections for elastic scattering of intermediate-energy positrons by argon atoms. In the present calculations of elastic scattering of electrons and positrons by argon, an attempt is made to use as similar (within physical consistency) potential for the two projectiles as is possible.

Elastic and total collisional scattering of *electrons* by argon has been given considerable attention, both experimentally as well as theoretically, during the past sixty years.[1,4—55] Webb[4] has summarized the electron-argon scattering results prior to 1935. The later experiments on integrated elastic and total collisional cross sections were performed by Aberth *et al.*[5] (15—25 eV), Golden and Bandel[6] (0.1—21.6 eV), Kauppila *et al.*[7] (1.5—15.7 eV), Wagenaar and de Heer[8] (25—750 eV), Wagenaar and de Heer[9] (20—100 eV), Kauppila *et al.*[10] (15—800 eV), Nickel *et al.*[11] (4—300 eV), Jost *et al.*[12] (0.08—54.423 eV), Ferch *et al.*[13] (0.08—20 eV), Charlton *et al.*[14] (2—50 eV), and Gus'kov *et al.*[15] (0.025—1.0 eV). The differential cross sections (DCS) for the elastic scattering of electrons by argon have been measured by Mehr[16] (5—1000 eV, 20°—155°), Schackert[17] (40—150 eV, 30°—150°), Bromberg[18] (200—700 eV, 2°—30°), Williams and Willis[19] (20—400 eV, 20°—150°), Jansen *et al.*[20] (100—3000 eV, 5°—55°), Lewis *et al.*[21] (15—200 eV, 20°—140°), Vušković and Kurepa[22] (60—150 eV, 5°—150°), DuBois and Rudd[23] (20—800 eV, 2°—150°), Gupta and Rees[24,25] (100 eV, 10°—150°), Williams[26] (0.5—20 eV, 15°—150°), Srivastava *et al.*[27] (3—100 eV, 20°—135°), Andrick[28] (1—20 eV, 0°—180°), Qing *et al.*[29] (10—50 eV, 40°—110°), and Filipović[30] (10—100 eV, 20°—150°). From experimental angular distribution measurements, integrated elastic cross sections have also been calculated in some cases. Semiempirical cross sections for elastic and inelastic scattering of electrons from argon in the energy range 20 to 3000 eV have been obtained by de Heer *et al.*[31] Momentum transfer cross sections for electron-argon scattering have been measured or derived from experimental parameters by McPherson *et al.*[32] (0.08—4 eV), Golovanivsky and Kabilan[33] (0.005—0.6 eV), and Haddad and O'Malley[34] (0—4 eV). Theoretical studies of electron- or positron-argon scattering are characterized by the method used as well as by the potential used in the calculations. Theoretical calculations for electron scattering by argon have been performed by Walker[35] and by Fink and Yates[36] using the relativistic approximation; Thompson,[37] Garbaty and LaBahn,[38] Yau *et al.*,[39] and Dasgupta and Bhatia[40] using the polarized orbital method; Fon *et al.*,[41] and Bell *et al.*[42] using the R-matrix method; Pindzola and Kelly,[43] Amusia *et al.*,[44] McCarthy *et al.*,[45] Joachain *et al.*,[46,47] and Staszewska *et al.*[48] using optical model potentials; Berg *et al.*[49] and Datta *et al.*[50] using model potentials; Khare and Shobha[51] using the first Born approximation; McEachran and Stauffer[52] using adiabatic exchange approximation; and Haberland *et al.*[53] using Kohn-Sham-type one-particle theory. Momentum transfer cross sections for electron-argon scattering are obtained by Frost and Phelps[54] from transport coefficients and by Milloy *et al.*[55] by a swarm technique.

All measurements of *positron* scattering by argon have

been made in the last decade or so. Measurements of total collisional cross sections for positron scattering from argon include those by Canter *et al.*[56] (2–400 eV), Jaduszliwer and Paul[57] (4–9 eV), Kauppila *et al.*[58] (0.4–18 eV), Coleman *et al.*[59] (2–960 eV), Griffith *et al.*[60] (30–800 eV), Tsai *et al.*[61] (25–300 eV), Brenton *et al.*[62] (200–1000 eV), Sinapius *et al.*[63] (1–6 eV), Coleman *et al.*[64] (2–50 eV), and Kauppila *et al.*[10] (15–800 eV). A recent summary of positron-gas scattering is given by Stein and Kauppila.[65] Measurements of the angular distribution for positron-argon elastic scattering have been made by Coleman and McNutt[66] (2.2–8.7 eV, 20°–60°) and by Hyder *et al.*[3] (100–300 eV, 30°–135°). On the theoretical side, positron-argon scattering calculations have been carried out by Joachain *et al.*[46] and Khare *et al.*[67] using optical model potentials; McEachran *et al.*[68] and McEachran and Stauffer[69] using the polarized orbital method; and Datta *et al.*[50] and Arifov and Zhuravleva[70] using a model potential. In the present study of elastic scattering of low- and intermediate-energy positrons and electrons from argon atoms, model static and Buckingham-type polarization potentials for the positron scattering and the same static (albeit with opposite sign) and polarization potentials along with an exchange potential for electron scattering have been used. The results of the present calculation are compared with the recent experimental observations of positrons and electrons elastically scattered from argon.

II. THEORY

Consider a projectile of charge e_p, with laboratory-frame impact energy E, being scattered elastically by a target with central potential $V(r)$. The scattering can be described by the radial part, $u_l(r)$, of the lth partial wave of the wave function which satisfies (in atomic units)

$$\left[\frac{d^2}{dr^2}-\frac{l(l+1)}{r^2}+2\mu[E-V(r)]\right]u_l(r)=0\ . \tag{1}$$

Here μ is the reduced mass of the system. The asymptotic form of the radial part of the wave function is

$$u_l(r)\underset{r\to\infty}{\to} kr[j_l(kr)-(\tan\delta_l)n_l(kr)]\ , \tag{2}$$

where $k^2=2\mu E$. j_l and n_l are the spherical Bessel functions of the first and the second kind, respectively. (For their numerical evaluation, see Appendix A.) For positron and electron impact, $\mu=1$. δ_l is the energy-dependent phase shift caused by the potential $V(r)$. From the values of the wave function at two adjacent points r and $r+h$ ($h\ll r$), in the asymptotic domain, one can extract the phase shift

$$\tan\delta_l=-\frac{(r+h)u_l(r)j_l(k(r+h))-ru_l(r+h)j_l(kr)}{ru_l(r+h)n_l(kr)-(r+h)u_l(r)n_l(k(r+h))}\ . \tag{3}$$

Various phase shifts are used to obtain the scattering amplitude as

$$f(\theta)=\frac{1}{2ik}\sum_{l=0}^{\infty}(2l+1)(e^{2i\delta_l}-1)P_l(\cos\theta)\ , \tag{4}$$

where θ is the scattering angle. Equation (1) is solved by using the Numerov procedure and the first L phase shifts are obtained exactly. L depends on the energy of the incident projectile. For large l ($>L$) the exact phase shifts δ_l are approximately equal to the Born phase shifts δ_{Bl},

$$\exp(i\delta_{Bl})\sin\delta_{Bl}\equiv T_{Bl}=-2k\int_0^{\infty}r^2j_l^2(kr)V(r)dr\ . \tag{5}$$

The typical values of L corresponding to the impact energies of 3 and 300 eV are 4 and 20, respectively.

The infinite sum in Eq. (4) is then approximated by

$$f(\theta)=\frac{1}{2ik}\sum_{l=0}^{L}(2l+1)[\exp(2i\delta_l)-1-\exp(2i\delta_{Bl})+1]\times P_l(\cos\theta)+f_B(\theta)\ , \tag{6}$$

where f_B is the scattering amplitude in the Born approximation. For a spherically symmetric potential $V(r)$,

$$f_B(\theta)=\frac{1}{2ik}\sum_{l=0}^{\infty}(2l+1)[\exp(2i\delta_{Bl})-1]P_l(\cos\theta)=-2\int_0^{\infty}r^2\frac{\sin(qr)}{qr}V(r)dr\ , \tag{7}$$

where $q=2k\sin(\theta/2)$ is the momentum transfer. The differential and the integrated elastic cross sections are

$$\frac{d\sigma}{d\Omega}=|f(\theta)|^2\ , \tag{8}$$

$$\sigma_l=2\pi\int_0^{\pi}\left[\frac{d\sigma}{d\Omega}\right]\sin\theta\,d\theta\ . \tag{9}$$

The transport cross sections (including the momentum transfer, $n=1$, cross section) are

$$\sigma^{(n)}=2\pi\int_0^{\pi}(1-\cos^n\theta)\left[\frac{d\sigma}{d\Omega}\right]\sin\theta\,d\theta\ . \tag{10}$$

TABLE I. Range of the values and the value used for the parameter d (in units of a_0) for various impact energies.

E (eV)	d (in units of a_0) Range of values	Value used
3	1.38–1.4	1.39
5	1.25–1.45	1.35
10	1.65–1.8	1.7
15	1.6 –1.8	1.6
20	1.7 –2.75	1.75
30	1.3 –1.7	1.65
40	1.35–1.7	1.6
50	1.3 –2.0	1.5
75	1.65–2.35	2.0
100	1.5 –2.5	2.0
150	1.5 –3.0	2.0
200	1.5 –3.0	2.0
250	1.5 –3.0	2.0
300	1.7 –3.0	2.0

The optical theorem

$$\sigma_I = \frac{4\pi}{k}\mathrm{Im}f(0) \tag{11}$$

is used as a self-consistent check on the present calculations. In the present calculations of elastic scattering of electrons and positrons by argon atoms, the potentials used are

$$V(r) = V_s(r) + V_p(r) \text{ for positron impact} \tag{12}$$

$$= V_s(r) + V_p(r) + V_{ex}(r) \text{ for electron impact .} \tag{13}$$

Here $V_s(r)$ is the static potential of the target atom, obtained by averaging over the motion of the target electrons:

$$V_s(\mathbf{r}) = \frac{Ze_p}{r} - \sum_{i=1}^{Z} e_p \int |\Psi(\mathbf{r}_1, \mathbf{r}_2, \ldots, \mathbf{r}_Z)|^2 \times \frac{1}{|\mathbf{r}-\mathbf{r}_i|} d\mathbf{r}_1 \cdots d\mathbf{r}_Z \ , \tag{14}$$

where Z is the nuclear charge of the target atom. $\Psi(\mathbf{r}_1, \ldots, \mathbf{r}_Z)$ is the antisymmetrized Hartree-Fock wave function of the target and is expanded in terms of the Slater-type orbitals:

$$\Phi_{\lambda p}(\mathbf{r}) = \sum_{i=1}^{M} A(\lambda,p,i) r^{n(p,i)-1} \exp[-\zeta(p,i)r] Y_{lm}(\hat{\mathbf{r}})$$

$$\equiv \phi_{\lambda p}(r) Y_{lm}(\hat{\mathbf{r}})$$

with

$$A(\lambda,p,i) = c(\lambda,p,i)[2\zeta(p,i)]^{n(p,i)+1/2} / \{[2n(p,i)]!\}^{1/2} . \tag{15}$$

The values of $c(\lambda,p,i)$, $\zeta(p,i)$, and $n(p,i)$ are taken from the tables of Clementi and Roetti.[71] Defining, for convenience,

$$\nu = n(p,i) + n(p,j), \quad z = \zeta(p,i) + \zeta(p,j), \quad a = A(\lambda,p,i)A(\lambda,p,j)\nu!, \quad s = z^{-\nu-1}, \quad m = [1/(t+1)! - 1/(t!\nu)]/z^{\nu-t} , \tag{16}$$

where i, j, and t are integers, the static potential for argon atom is given by

$$V_s(r) = e_p \sum_{\lambda=1}^{N} \sum_{p=0}^{\lambda-1} N_{\lambda p} \sum_{i=1}^{M} \sum_{j=1}^{M} a \exp(-zr) \left[\frac{s}{r} + \sum_{t=0}^{\nu-2} m r^t \right] , \tag{17}$$

where N is the number of occupied shells in the atom and $N_{\lambda p}$ is the number of electrons in the orbital (λ,p). V_p is taken to be a model polarization potential of the Buckingham type,

$$V_p(r) = -\tfrac{1}{2}\alpha r^2/(r^2+d^2)^3 , \tag{18}$$

where α is the static dipole polarizability. d is an energy-dependent adjustable parameter determined by fitting the calculated differential and integrated cross sections for the elastic scattering of electrons by argon atoms with the experimental values of the same at a particular energy. The same value of d is then used for positron-argon scattering calculations at that energy. The values of the parameter d for various impact energies are given in Table I. Khare *et al.*,[67,72] who have used a very similar polarization potential, have expressed the parameter d as a linear function of k in their work. The exchange potential, $V_{ex}(r)$, for a closed-shell atom is taken to be[73]

$$V_{ex}(r) = \tfrac{1}{2}\left[[E - V_D(r)] - \left[[E - V_D(r)]^2 + \sum_{\lambda=1}^{N} \sum_{p=0}^{\lambda-1} N_{\lambda p} |\phi_{\lambda p}(r)|^2 \right]^{1/2} \right] , \tag{19}$$

where V_D is the direct interaction potential, namely, $V_D = V_s + V_p$. $\phi_{\lambda p}(r)$ is the radial part of the Slater-type orbital as in Eq. (15). $V_{ex}(r)$ is a shorter range and much weaker potential than the static potential. Hence it is excluded from the computation of the phase shifts of higher partial waves using the Born approximation. For the polarization potential, the integral for the lth Born phase shift, Eq. (5), defined by T_{pBl}, is (for its derivation see Appendix B)

$$T_{pBl} = \tfrac{1}{4}\alpha k^2 \{ -(2l+3) i_{l+1}(kd) k_l(kd) + \pi(2l+3)/(4k^2d^2) - [kd + (2l+1)(2l+3)/(2kd)] i_l(kd) k_l(kd) + kd i_{l+1}(kd) k_{l+1}(kd) \} , \tag{20}$$

where i_l and k_l are the modified spherical Bessel functions of the first and the third kind, respectively. (For their numerical evaluation see Appendix A.) The Born amplitude, Eq. (7), for the polarization potential defined above, is

$$f_{Bp} = \pi\alpha(3 - qd)\exp(-qd)/(16d) . \tag{21}$$

For the static potential, the lth Born phase shift, Eq. (5), defined to be T_{sBl}, is (for details see Appendix C)

$$T_{sBl} = -\frac{e_p}{k} \sum_{\lambda=1}^{N} \sum_{p=0}^{\lambda-1} N_{\lambda p} \sum_{i=1}^{M} \sum_{j=1}^{M} a \left[sQ_l \left[1 + \frac{z^2}{2k^2} \right] + \sum_{t=0}^{\nu-2} (-1)^{t+1} m \frac{d^{t+1}}{dz^{t+1}} Q_l \left[1 + \frac{z^2}{2k^2} \right] \right] , \tag{22}$$

where ν, z, a, s, and m are defined in (16). Q_l is the Legendre function of the second kind. The corresponding Born scattering amplitude, f_{Bs}, is

$$f_{Bs} = -2e_p \sum_{\lambda=1}^{N} \sum_{p=0}^{\lambda-1} N_{\lambda p} \sum_{i=1}^{M} \sum_{j=1}^{M} a \left[\frac{s}{z^2+q^2} + \sum_{t=0}^{\nu-2} (-1)^{t+1} m \frac{d^{t+1}}{dz^{t+1}} \frac{1}{z^2+q^2} \right] . \quad (23)$$

For a given impact energy, the polarization potential provides the major contribution and the static potential a non-negligible contribution to the phase shifts of higher partial waves especially for the case of positron impact. The reason is that due to the opposite nature of the static and polarization interactions for the positron case, the first part of the scattering amplitude obtained from the first L exact phase shifts [see Eq. (6)] is smaller for positron impact than for electron impact and thus the relative contribution of the Born-approximation part with static interaction is more significant for positron impact than for electron impact.

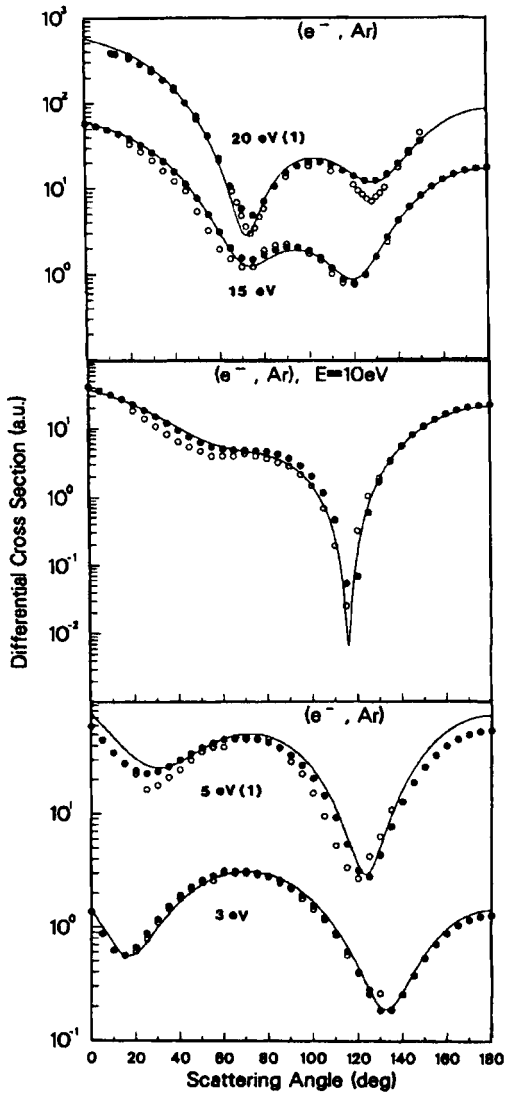

FIG. 1. Differential cross sections for the elastic scattering of electrons by argon at various impact energies. Solid lines are the present theoretical curves. The number in parenthesis following an energy value indicates the power of ten by which the cross section values are multiplied. The experimental values are open circles, Ref. 27 for 3, 5, 10, and 15 eV and Ref. 19 for 20 eV; closed circles, Ref. 28 for 3, 5, 10, and 15 eV and Ref. 23 for 20 eV.

III. RESULTS AND DISCUSSION

The differential and integrated cross sections for the elastic scattering of electrons from argon are shown in

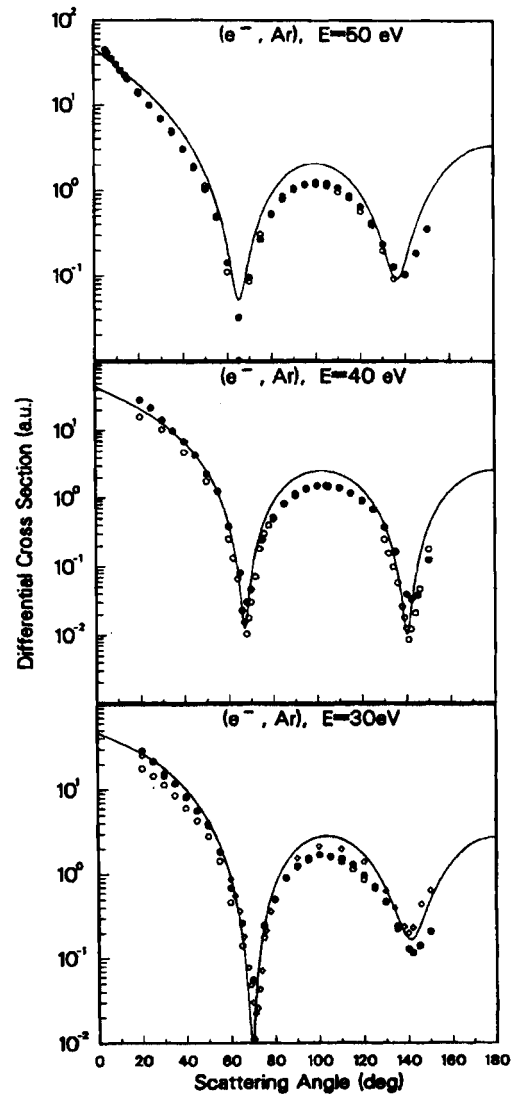

FIG. 2. Same as Fig. 1 except the experimental values are open circles, Ref. 27 for 30 and 50 eV and Ref. 19 for 40 eV; closed circles, Ref. 30 for 30 and 40 eV and Ref. 23 for 50 eV; diamonds, Ref. 19 for 30 eV.

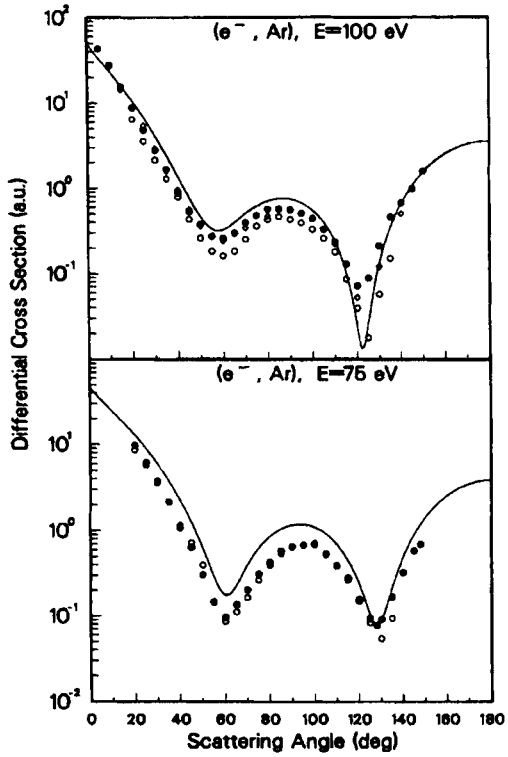

FIG. 3. Same as Fig. 1 except the experimental values are open circles, Ref. 27 for 75 and 100 eV; closed circles, Ref. 30 for 75 eV and Ref. 22 for 100 eV; diamonds, Ref. 25 for 100 eV.

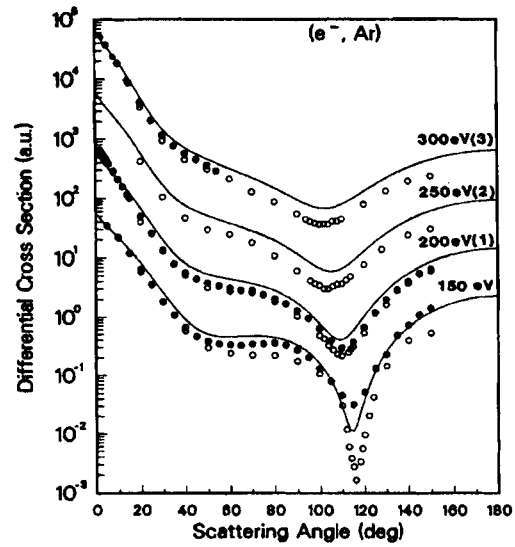

FIG. 4. Same as Fig. 1 except the experimental values are open circles, Ref. 19 for 150, 200, 250, and 300 eV; closed circles, Ref. 22 for 150 eV, Ref. 23 for 200 eV, and Ref. 20 for 300 eV; diamonds, Ref. 18 for 300 eV.

Figs. 1–4. The single adjustable parameter d in the polarization potential has been varied, for each impact energy, to fit, as closely as possible, the experimentally observed differential as well as integrated cross sections for elastic scattering of electrons from argon. It was noticed that a finite range of values of d could be used for such a fitting procedure. Table I gives the range of values of d along with the final value of d used for computing the present cross sections. It is seen by observing the size of the range of values of d from Table I that the cross sections are more sensitive to the value of d at lower energies

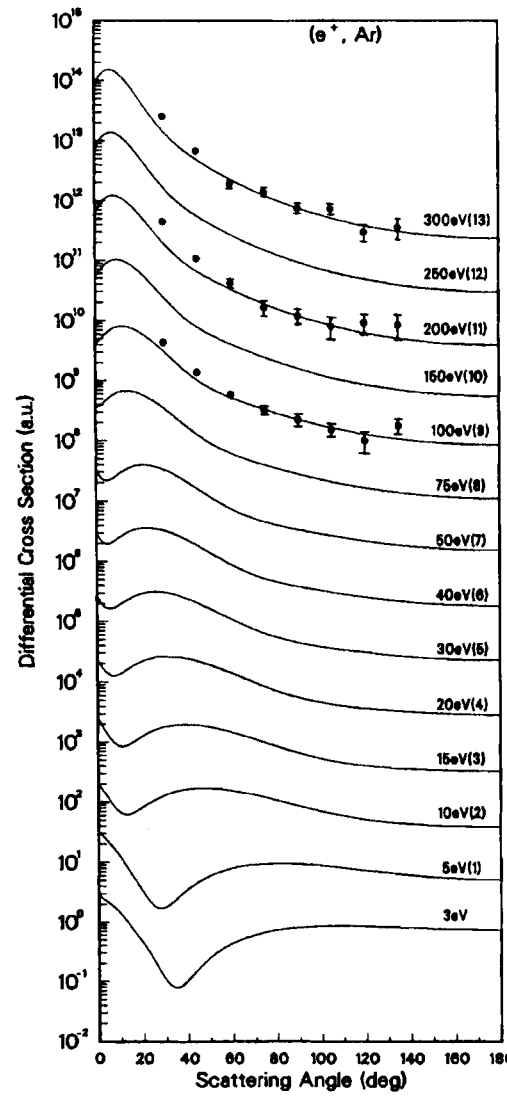

FIG. 5. Differential cross sections for the elastic scattering of positrons by argon at various impact energies. Solid lines are the present theoretical curves. The number in parentheses following an energy value indicates the power of ten by which the cross section values are multiplied. The experimental values are from Ref. 3.

TABLE II. Differential and integrated cross sections ($a_0^2\,sr^{-1}$) for elastic scattering of *electrons* from argon at $E=3$–300 eV.

θ (deg) \ E (eV)	3	5	10	15	20	30	40
0	0.147[1][a]	0.760[1]	0.377[2]	0.602[2]	0.571[2]	0.472[2]	0.460[2]
5	0.102[1]	0.608[1]	0.341[2]	0.557[2]	0.523[2]	0.409[2]	0.373[2]
10	0.717	0.481[1]	0.300[2]	0.509[2]	0.476[2]	0.359[2]	0.308[2]
15	0.560	0.379[1]	0.262[2]	0.455[2]	0.426[2]	0.312[2]	0.254[2]
20	0.585	0.311[1]	0.224[2]	0.396[2]	0.371[2]	0.267[2]	0.208[2]
25	0.742	0.271[1]	0.189[2]	0.335[2]	0.314[2]	0.222[2]	0.166[2]
30	0.101[1]	0.257[1]	0.156[2]	0.274[2]	0.256[2]	0.179[2]	0.129[2]
35	0.133[1]	0.265[1]	0.127[2]	0.215[2]	0.200[2]	0.138[2]	0.955[1]
40	0.170[1]	0.291[1]	0.103[2]	0.161[2]	0.149[2]	0.101[2]	0.673[1]
45	0.207[1]	0.330[1]	0.843[1]	0.115[2]	0.104[2]	0.685[1]	0.440[1]
50	0.242[1]	0.377[1]	0.699[1]	0.777[1]	0.673[1]	0.422[1]	0.257[1]
55	0.272[1]	0.424[1]	0.599[1]	0.496[1]	0.391[1]	0.225[1]	0.125[1]
60	0.295[1]	0.466[1]	0.534[1]	0.302[1]	0.196[1]	0.916	0.423
65	0.310[1]	0.498[1]	0.491[1]	0.187[1]	0.808	0.198	0.492[−1]
70	0.315[1]	0.513[1]	0.461[1]	0.134[1]	0.322	0.110[−1]	0.619[−1]
75	0.310[1]	0.510[1]	0.433[1]	0.125[1]	0.341	0.238	0.368
80	0.295[1]	0.488[1]	0.397[1]	0.140[1]	0.686	0.739	0.859
85	0.273[1]	0.447[1]	0.350[1]	0.164[1]	0.118[1]	0.137[1]	0.142[1]
90	0.243[1]	0.390[1]	0.290[1]	0.183[1]	0.168[1]	0.198[1]	0.193[1]
95	0.208[1]	0.322[1]	0.220[1]	0.187[1]	0.205[1]	0.247[1]	0.231[1]
100	0.171[1]	0.248[1]	0.145[1]	0.176[1]	0.224[1]	0.275[1]	0.250[1]
105	0.134[1]	0.177[1]	0.771	0.151[1]	0.222[1]	0.279[1]	0.247[1]
110	0.990	0.113[1]	0.252	0.121[1]	0.204[1]	0.259[1]	0.223[1]
115	0.685	0.643	0.120[−1]	0.951	0.174[1]	0.219[1]	0.183[1]
120	0.446	0.358	0.150	0.864	0.144[1]	0.168[1]	0.134[1]
125	0.281	0.311	0.741	0.106[1]	0.122[1]	0.114[1]	0.843
130	0.199	0.519	0.182[1]	0.164[1]	0.117[1]	0.663	0.412
135	0.197	0.980	0.339[1]	0.264[1]	0.137[1]	0.321	0.119
140	0.269	0.166[1]	0.539[1]	0.407[1]	0.185[1]	0.172	0.103[−1]
145	0.403	0.252[1]	0.773[1]	0.586[1]	0.261[1]	0.234	0.101
150	0.581	0.350[1]	0.103[2]	0.793[1]	0.358[1]	0.495	0.375
155	0.781	0.451[1]	0.128[2]	0.101[2]	0.469[1]	0.912	0.791
160	0.985	0.548[1]	0.152[2]	0.122[2]	0.583[1]	0.141[1]	0.128[1]
165	0.117[1]	0.633[1]	0.173[2]	0.141[2]	0.688[1]	0.192[1]	0.177[1]
170	0.131[1]	0.700[1]	0.190[2]	0.156[2]	0.773[1]	0.236[1]	0.219[1]
175	0.141[1]	0.742[1]	0.200[2]	0.166[2]	0.828[1]	0.265[1]	0.247[1]
180	0.144[1]	0.755[1]	0.204[2]	0.169[2]	0.847[1]	0.275[1]	0.257[1]
σ_I	0.207[2]	0.393[2]	0.763[2]	0.866[2]	0.728[2]	0.511[2]	0.396[2]

θ (deg) \ E (eV)	50	75	100	150	200	250	300
0	0.488[2]	0.474[2]	0.505[2]	0.555[2]	0.595[2]	0.630[2]	0.661[2]
5	0.374[2]	0.332[2]	0.334[2]	0.337[2]	0.341[2]	0.344[2]	0.347[2]
10	0.293[2]	0.244[2]	0.232[2]	0.218[2]	0.208[2]	0.201[2]	0.194[2]
15	0.229[2]	0.180[2]	0.161[2]	0.138[2]	0.123[2]	0.111[2]	0.102[2]
20	0.177[2]	0.129[2]	0.107[2]	0.824[1]	0.679[1]	0.581[1]	0.509[1]
25	0.134[2]	0.896[1]	0.685[1]	0.470[1]	0.363[1]	0.300[1]	0.259[1]
30	0.986[1]	0.597[1]	0.419[1]	0.262[1]	0.198[1]	0.166[1]	0.147[1]
35	0.699[1]	0.380[1]	0.246[1]	0.149[1]	0.119[1]	0.105[1]	0.963
40	0.471[1]	0.228[1]	0.140[1]	0.911	0.809	0.760	0.713
45	0.294[1]	0.126[1]	0.789	0.632	0.627	0.605	0.564
50	0.162[1]	0.629	0.465	0.508	0.532	0.506	0.460
55	0.729	0.290	0.332	0.463	0.476	0.435	0.382
60	0.221	0.175	0.324	0.457	0.437	0.378	0.319
65	0.516[−1]	0.228	0.394	0.467	0.404	0.329	0.267
70	0.162	0.395	0.504	0.475	0.370	0.283	0.223
75	0.475	0.621	0.620	0.470	0.330	0.239	0.183

TABLE II. (*Continued*).

θ (deg) \ E (eV)	50	75	100	150	200	250	300
80	0.902	0.853	0.713	0.445	0.282	0.195	0.149
85	0.135[1]	0.105[1]	0.760	0.397	0.229	0.154	0.119
90	0.174[1]	0.116[1]	0.749	0.327	0.173	0.117	0.948[−1]
95	0.199[1]	0.118[1]	0.678	0.244	0.121	0.869[−1]	0.778[−1]
100	0.208[1]	0.109[1]	0.555	0.158	0.769[−1]	0.668[−1]	0.691[−1]
105	0.198[1]	0.921	0.400	0.818[−1]	0.485[−1]	0.593[−1]	0.697[−1]
110	0.172[1]	0.693	0.239	0.286[−1]	0.412[−1]	0.668[−1]	0.804[−1]
115	0.135[1]	0.449	0.103	0.113[−1]	0.592[−1]	0.904[−1]	0.101
120	0.925	0.238	0.236[−1]	0.401[−1]	0.105	0.131	0.133
125	0.532	0.104	0.263[−1]	0.121	0.180	0.187	0.173
130	0.237	0.869[−1]	0.130	0.257	0.282	0.257	0.221
135	0.971[−1]	0.210	0.343	0.444	0.408	0.339	0.276
140	0.145	0.482	0.662	0.676	0.552	0.429	0.334
145	0.387	0.889	0.107[1]	0.939	0.706	0.524	0.395
150	0.799	0.140[1]	0.154[1]	0.122[1]	0.864	0.617	0.454
155	0.133[1]	0.198[1]	0.204[1]	0.150[1]	0.102[1]	0.706	0.509
160	0.192[1]	0.256[1]	0.252[1]	0.176[1]	0.115[1]	0.786	0.558
165	0.249[1]	0.309[1]	0.295[1]	0.198[1]	0.127[1]	0.853	0.599
170	0.296[1]	0.352[1]	0.329[1]	0.215[1]	0.136[1]	0.903	0.630
175	0.327[1]	0.379[1]	0.351[1]	0.226[1]	0.142[1]	0.934	0.649
180	0.338[1]	0.388[1]	0.358[1]	0.230[1]	0.144[1]	0.945	0.655
σ_1	0.333[2]	0.234[2]	0.192[2]	0.150[2]	0.128[2]	0.114[2]	0.103[2]

[a]The notation $a[b]$ means $a \times 10^b$.

than at higher energies. The reason possibly is that the polarization interaction plays a more significant role at lower energies. It was also noticed that variation of d has a significant effect on the location of the minima and the maxima of the DCS curves and on the value of the DCS at those locations, especially at low energies. Variation of d also affected the DCS in the forward direction at all energies. Hence the DCS curves could be moved up and down near the forward direction by changing the value of d whereas the shape of the DCS curves at higher angles stayed about the same.

Within the range of values of d, shown in Table I for various electron-impact energies, the computed DCS curves and the integrated elastic cross sections remain close to the corresponding experimentally measured values. The value of d that, in our judgment, gave the best fitting was used for final computation of differential and integrated elastic cross sections for the scattering of both the electrons as well as the positrons. The DCS curves in the forward direction for positron impact are more sensitive to the value of d than the corresponding curves for electron impact due to the tendency of cancellation between the static and polarization interactions for the positrons. The differential cross sections for the elastic scattering of positrons from argon are shown in Fig. 5. Numerical values of the differential and integrated elastic cross sections for the scattering of electrons and positrons from argon are provided in Tables II and III.

A comparison of the various cross sections calculated here, for *electron* scattering, with corresponding measured values is given in Figs. 1–4 and in Tables IV and V. The calculated DCS curves for elastic scattering of electrons from argon are in good agreement with the measured values of Srivastava *et al.*,[27] Andrick,[28] DuBois and Rudd,[23] and Filipović[30] at lower energies (<50 eV) and with Vušković and Kurepa,[22] and DuBois and Rudd[23] at higher energies ($100 \leq E \leq 200$ eV). However, the agreement with Srivastava *et al.*[27] and Filipović[30] at larger angles becomes progressively poorer as the electron-impact energy becomes large. The differential cross sections measured by Williams and Willis[19] are almost always lower than our calculated cross sections at the minimum points. The integrated elastic cross sections given in Table IV are consistent with the available experimental values except with those of Srivastava *et al.*[27] which are lower than our calculated values. The transport cross sections, which represent the moments of $1-(\cos\theta)^n$, and which are related to the momentum transfer or diffusion cross section (for $n=1$), viscosity and thermal conductivity cross section (for $n=2$), etc.,[74] for both electrons and positrons are tabulated in Table V. Comparison in Table V of the present momentum transfer cross sections for the electron-argon system with the corresponding experimental values shows reasonable agreement except with the results of Ref. 27. Phase shifts of the seven lowest partial waves ($l=0$–6) for various impact energies of electrons and positrons are presented in Table VI and compare favorably with the available measured values.

The DCS curves for the elastic scattering of *positrons* by argon at various energies are shown in Fig. 5. These

TABLE III. Differential and integrated cross sections ($a_0^2\,sr^{-1}$) for elastic scattering of *positrons* from argon at $E = 3-300$ eV.

θ (deg) \ E (eV)	3	5	10	15	20	30	40
0	0.295[1][a]	0.335[1]	0.212[1]	0.263[1]	0.239[1]	0.276[1]	0.302[1]
5	0.209[1]	0.210[1]	0.114[1]	0.127[1]	0.134[1]	0.167[1]	0.199[1]
10	0.140[1]	0.122[1]	0.676	0.875	0.135[1]	0.193[1]	0.252[1]
15	0.795	0.626	0.651	0.983	0.176[1]	0.253[1]	0.325[1]
20	0.441	0.321	0.832	0.128[1]	0.220[1]	0.299[1]	0.365[1]
25	0.220	0.189	0.109[1]	0.160[1]	0.251[1]	0.318[1]	0.364[1]
30	0.108	0.183	0.133[1]	0.185[1]	0.263[1]	0.309[1]	0.332[1]
35	0.795[−1]	0.252	0.153[1]	0.198[1]	0.259[1]	0.281[1]	0.284[1]
40	0.107	0.364	0.165[1]	0.201[1]	0.242[1]	0.244[1]	0.232[1]
45	0.170	0.488	0.171[1]	0.195[1]	0.218[1]	0.204[1]	0.184[1]
50	0.256	0.615	0.170[1]	0.182[1]	0.191[1]	0.167[1]	0.143[1]
55	0.348	0.724	0.165[1]	0.166[1]	0.164[1]	0.135[1]	0.112[1]
60	0.445	0.819	0.156[1]	0.148[1]	0.138[1]	0.109[1]	0.888
65	0.536	0.890	0.144[1]	0.131[1]	0.116[1]	0.888	0.722
70	0.617	0.937	0.132[1]	0.114[1]	0.981	0.737	0.605
75	0.689	0.968	0.120[1]	0.990	0.833	0.626	0.523
80	0.747	0.976	0.108[1]	0.861	0.716	0.545	0.464
85	0.796	0.973	0.967	0.753	0.626	0.485	0.419
90	0.830	0.954	0.869	0.665	0.556	0.441	0.384
95	0.855	0.929	0.782	0.594	0.504	0.407	0.355
100	0.870	0.896	0.707	0.538	0.464	0.379	0.330
105	0.877	0.860	0.645	0.493	0.432	0.357	0.309
110	0.879	0.823	0.592	0.459	0.408	0.337	0.289
115	0.873	0.783	0.549	0.432	0.388	0.320	0.272
120	0.865	0.746	0.514	0.411	0.371	0.304	0.257
125	0.853	0.709	0.486	0.394	0.357	0.291	0.244
130	0.841	0.676	0.463	0.381	0.345	0.279	0.232
135	0.826	0.645	0.445	0.370	0.335	0.268	0.222
140	0.812	0.618	0.431	0.361	0.326	0.259	0.213
145	0.799	0.594	0.420	0.354	0.318	0.251	0.206
150	0.785	0.572	0.411	0.348	0.311	0.243	0.200
155	0.775	0.557	0.404	0.343	0.305	0.238	0.195
160	0.763	0.541	0.399	0.339	0.300	0.233	0.191
165	0.757	0.531	0.395	0.336	0.297	0.230	0.188
170	0.750	0.523	0.392	0.334	0.294	0.227	0.186
175	0.747	0.518	0.391	0.333	0.293	0.226	0.184
180	0.749	0.520	0.390	0.332	0.292	0.225	0.184
σ_t	0.842[1]	0.927[1]	0.118[2]	0.113[2]	0.117[2]	0.109[2]	0.104[2]

θ (deg) \ E (eV)	50	75	100	150	200	250	300
0	0.334[1]	0.365[1]	0.426[1]	0.532[1]	0.623[1]	0.704[1]	0.777[1]
5	0.219[1]	0.493[1]	0.640[1]	0.903[1]	0.113[2]	0.132[2]	0.149[2]
10	0.286[1]	0.653[1]	0.809[1]	0.104[2]	0.119[2]	0.129[2]	0.136[2]
15	0.364[1]	0.680[1]	0.778[1]	0.875[1]	0.901[1]	0.892[1]	0.865[1]
20	0.396[1]	0.602[1]	0.630[1]	0.618[1]	0.573[1]	0.522[1]	0.473[1]
25	0.379[1]	0.477[1]	0.459[1]	0.397[1]	0.339[1]	0.292[1]	0.255[1]
30	0.331[1]	0.352[1]	0.314[1]	0.248[1]	0.202[1]	0.171[1]	0.148[1]
35	0.270[1]	0.251[1]	0.211[1]	0.159[1]	0.129[1]	0.110[1]	0.958
40	0.211[1]	0.177[1]	0.144[1]	0.109[1]	0.894	0.768	0.673
45	0.162[1]	0.127[1]	0.104[1]	0.798	0.665	0.571	0.497
50	0.123[1]	0.950	0.789	0.620	0.517	0.439	0.377
55	0.947	0.746	0.632	0.500	0.411	0.344	0.292
60	0.751	0.612	0.524	0.411	0.333	0.275	0.230
65	0.616	0.519	0.445	0.343	0.273	0.222	0.184
70	0.524	0.450	0.383	0.289	0.226	0.182	0.150
75	0.459	0.395	0.332	0.245	0.190	0.152	0.124
80	0.410	0.350	0.290	0.211	0.161	0.128	0.104

TABLE III. (*Continued*).

θ (deg) \ E (eV)	50	75	100	150	200	250	300
85	0.372	0.312	0.256	0.183	0.138	0.109	0.886[−1]
90	0.340	0.280	0.227	0.160	0.120	0.943[−1]	0.762[−1]
95	0.313	0.252	0.202	0.141	0.106	0.824[−1]	0.664[−1]
100	0.290	0.229	0.182	0.126	0.937[−1]	0.728[−1]	0.584[−1]
105	0.269	0.209	0.166	0.114	0.839[−1]	0.649[−1]	0.520[−1]
110	0.250	0.192	0.151	0.103	0.757[−1]	0.584[−1]	0.467[−1]
115	0.234	0.178	0.140	0.944[−1]	0.690[−1]	0.530[−1]	0.423[−1]
120	0.220	0.166	0.130	0.871[−1]	0.633[−1]	0.485[−1]	0.387[−1]
125	0.208	0.156	0.121	0.808[−1]	0.586[−1]	0.448[−1]	0.357[−1]
130	0.197	0.147	0.114	0.756[−1]	0.546[−1]	0.417[−1]	0.332[−1]
135	0.188	0.140	0.108	0.712[−1]	0.513[−1]	0.391[−1]	0.311[−1]
140	0.180	0.133	0.103	0.675[−1]	0.485[−1]	0.369[−1]	0.293[−1]
145	0.174	0.128	0.982[−1]	0.644[−1]	0.462[−1]	0.351[−1]	0.279[−1]
150	0.168	0.124	0.946[−1]	0.619[−1]	0.443[−1]	0.336[−1]	0.267[−1]
155	0.164	0.120	0.917[−1]	0.598[−1]	0.427[−1]	0.325[−1]	0.258[−1]
160	0.160	0.117	0.894[−1]	0.582[−1]	0.415[−1]	0.315[−1]	0.250[−1]
165	0.158	0.115	0.877[−1]	0.569[−1]	0.406[−1]	0.308[−1]	0.245[−1]
170	0.156	0.114	0.864[−1]	0.561[−1]	0.400[−1]	0.303[−1]	0.241[−1]
175	0.155	0.113	0.857[−1]	0.556[−1]	0.396[−1]	0.300[−1]	0.238[−1]
180	0.155	0.113	0.855[−1]	0.554[−1]	0.395[−1]	0.299[−1]	0.238[−1]
σ_I	0.973[1]	0.102[2]	0.956[1]	0.861[1]	0.791[1]	0.736[1]	0.690[1]

[a]The notation $a[b]$ means $a \times 10^b$.

curves show a minimum at low energies which shifts toward the forward direction with increasing impact energy. The increasing depth of this minimum on lowering the impact energy suggests the existence of the critical point for the positron-argon system. The critical points represent the points of minimum scattering, where a small change in either the incident projectile energy or the scattering angle is associated with an appreciable increase in the differential scattering cross section. The low-energy critical points for various positron–rare-gas-atom systems have been predicted by Wadehra *et al.*[75] So far the measurements of the angular distributions of elastic

TABLE IV. Comparison of calculated integrated elastic cross sections (in units of a_0^2) with the experimental values.

Projectile	E (eV)	Present value of σ_I	Experimental value of σ_I
e^-	3	20.66	20.83(7),[a] 19.48(12), 17.3(13), 20.64(14), 20.12(26), 19.65(27), 20.51(28)
	5	39.31	33.95(7), 32.1(11), 32.59(12), 30.87(13), 36.76(14), 36.09(26), 30.02(27), 34.73(28)
	10	76.33	70.75(10), 73.47(11), 74.33(12), 67.54(13), 69.3(14), 83.4(26), 64.32(27), 77.29(28)
	15	86.57	85.5(26), 75.04(27), 85.48(28)
	20	72.79	71.31(19), 68.4(23), 70.65(26), 44.67(27), 71.18(28)
	30	51.08	47.21(19)
	40	39.61	32.28(19)
	50	33.28	26.48(19), 25.61(23), 21.8(27)
	75	23.37	14.29(27)
	100	19.21	18.66(19), 16.51(20), 17.33(22), 17.1(23), 18.04(24), 9.29(27)
	150	15.02	11.86(19), 13.21(20), 13.33(22), 14.83(24)
	200	12.8	11.51(18), 9.81(19), 10.9(23), 12.68(24)
	300	10.32	8.74(18), 7.82(19), 8.81(20), 10.19(24)
e^+	3	8.42	12.57(56), 9.11(58), 8.56(64)
	5	9.27	12.56(56), 10.8(57), 9.68(58), 8.73(64)

[a]The notation $a(b)$ for experimental values of σ_I means the measured value of a taken from Ref. b.

TABLE V. The higher transport cross sections $\sigma^{(n)}$ (in units of a_0^2) and comparison of $\sigma^{(1)}$ with the experimental values.

Projectile	E (eV)	$\sigma^{(4)}$	$\sigma^{(3)}$	$\sigma^{(2)}$	$\sigma^{(1)}$	Experimental momentum transfer, $\sigma^{(1)}$
e^-	3	18.19	19.41	15.89	16.56	16.72(26),[a] 14.65(27), 16.08(28)
	5	30.45	38.97	25.98	34.67	32.45(26), 22.87(27), 29.5(28)
	10	42.15	66.37	31.61	58.97	67.65(26), 53.6(27), 62.4(28)
	15	40.84	58.57	28.41	49.56	51.2(26), 53.6(27), 51.28(28)
	20	34.83	41.82	24.44	33.65	33.66(26), 23.58(27), 34.8(28)
	30	26.18	26.52	19.40	21.33	13.22(27)
	40	20.20	20.82	15.38	17.49	
	50	16.12	18.05	12.38	15.67	8.58(27)
	75	9.98	13.40	7.60	11.90	6.79(27)
	100	7.39	11.03	5.48	9.78	5.72(27)
	150	5.24	7.96	3.74	6.95	
	200	4.26	6.08	2.99	5.22	
	250	3.63	4.86	2.53	4.09	
	300	3.16	4.01	2.19	3.31	
e^+	3	6.87	9.02	5.89	9.71	
	5	7.87	9.39	6.80	9.44	
	10	9.67	10.40	8.01	8.95	
	15	8.85	9.33	7.15	7.64	
	20	8.63	8.92	6.79	7.01	
	30	7.51	7.62	5.78	5.79	
	40	6.73	6.73	5.10	5.00	
	50	6.04	5.98	4.55	4.38	
	75	5.38	5.19	3.95	3.63	
	100	4.62	4.40	3.36	2.30	
	150	3.64	3.40	2.60	2.22	
	200	3.01	2.77	2.12	1.74	
	250	2.56	2.33	1.77	1.43	
	300	2.22	2.00	1.52	1.20	

[a]The notation $a(b)$ for experimental values of $\sigma^{(1)}$ means the measured value of a taken from Ref. b.

scattering of positrons by argon have been made only for a limited range of energies. The only available measured relative values of differential cross sections of Hyder *et al.*[3] at energies 100, 200, and 300 eV, have been normalized to the present calculated DCS curves at 90°. In this energy range, other calculations of elastic cross sections are those of McEachran and Stauffer[69] using the polarized orbital method and some limited results by Joachain[47] using the optical model potential. At higher energies and at larger angles the present calculations of DCS agree with those of McEachran and Stauffer and with the measurements of Hyder *et al.* When normalized separately at 90°, the measurements of Hyder *et al.* at 300 eV agree well both with the present calculation as well as with the calculations of Joachain.[47] At low energies and near the forward scattering direction, where unfortunately no experimental information for positron-argon elastic scattering is available, our DCS curves differ significantly from the calculated results of McEachran and Stauffer. It would certainly be worthwhile to carry out experiments on the elastic differential scattering of positrons by argon in this energy and angular range. For positron energies smaller than the positronium formation threshold in Ar (8.96 eV), the integrated elastic cross sections are compared in Table IV with the measured total positron-argon collisional cross sections. Higher transport cross sections and the lowest seven phase shifts for positron-argon elastic scattering are given in Tables V and VI, respectively. No comparison of these numbers is possible due to the lack of measurements of these quantities.

Finally, an attempt was made to obtain the cross sections for the elastic scattering of ultralow ($\lesssim 2.5$ eV) energy electrons and positrons by argon. In this energy range, no experimental numerical values of differential cross sections for electron impact are available. Thus it was not possible to obtain the low-energy parameters such as the scattering length and effective range for the positron-argon system using the present procedure.

In the present paper we have obtained various cross sections—differential, integrated, momentum transfer, etc.—and the corresponding phase shifts for the elastic scattering of positrons and electrons by argon. These cross sections compare favorably with the recent measurements of elastic differential scattering of intermediate-energy positrons by argon. With the anticipation that similar measurements will be made for other rare-gas targets in the near future, we are presently calculating the cross sections for the elastic scattering of low- and intermediate-energy positrons by He, Ne, Kr, and Xe by a similar procedure.

TABLE VI. Phase shifts (rad) of the first seven partial waves for elastic scattering of electrons and positrons by argon.

Projectile	E (eV)	$l=0$	$l=1$	$l=2$	$l=3$	$l=4$	$l=5$	$l=6$
e^-	3	−0.490	−0.132	0.130	0.0241	0.0106	0.0057	0.003 46
		−0.457	−0.134	0.142	0.021(26)[a]			
		−0.548	−0.140	0.125	0.035(27)			
		−0.493	−0.142	0.120	0.025(28)			
	5	−0.747	−0.272	0.306	0.042	0.0175	0.0094	0.0057
		−0.685	−0.205	0.317	0.031(26)			
		−0.747	−0.256	0.254	0.102(27)			
		−0.733	−0.277	0.260	0.044(28)			
	10	−1.283	−0.688	0.751	0.084	0.0321	0.0172	0.0106
		−1.098	−0.528	0.936	0.093(26)			
		−1.243	−0.430	0.805	0.171(27)			
		−1.143	−0.562	0.840	0.10(28)			
	15	−1.569	−0.867	1.131	0.140	0.0497	0.0255	0.0156
		−1.394	−0.750	1.451	0.154(26)			
		−1.365	−0.506	1.593	0.2(27)			
		−1.443	−0.782	1.39	0.165(28)			
	20	−1.826	−1.064	1.519	0.186	0.064	0.032	0.0194
		−1.653	−0.935	1.747	0.241(26)			
		−1.818	−0.871	1.679	0.262(27)			
		−1.683	−0.962	1.670	0.232(28)			
	30	−2.154	−1.296	1.817	0.306	0.104	0.0496	0.0288
	40	−2.40	−1.47	1.929	0.421	0.147	0.0682	0.0386
	50	−2.583	−1.595	2.008	0.539	0.196	0.0909	0.0503
	75	0.122	1.207	−1.184	0.645	0.250	0.116	0.0622
	100	−0.146	1.014	−1.166	0.773	0.330	0.159	0.0858
	150	−0.532	0.735	−1.168	0.929	0.460	0.241	0.135
	200	−0.809	0.535	−1.185	1.013	0.552	0.311	0.182
	250	−1.027	0.38	−1.207	1.064	0.619	0.368	0.225
	300	−1.205	0.253	−1.229	1.096	0.668	0.415	0.263
e^+	3	−0.334	0.0839	0.0528	0.0219	0.0105	0.005 72	0.003 46
	5	−0.496	0.0505	0.0703	0.0341	0.0169	0.009 39	0.005 72
	10	−0.878	−0.139	0.0455	0.0456	0.0278	0.0167	0.0106
	15	−1.06	−0.251	0.0173	0.0509	0.0368	0.0235	0.0152
	20	−1.245	−0.384	−0.0427	0.0371	0.0378	0.027	0.0185
	30	−1.455	−0.545	−0.126	0.0132	0.0385	0.0335	0.0248
	40	1.529	−0.674	−0.206	−2.081	0.0306	0.0354	0.0291
	50	1.423	−0.765	−0.267	−0.0506	0.0217	0.036	0.0326
	75	1.115	−1.044	−0.487	−0.196	−0.0598	−0.0038	0.0154
	100	0.967	−1.185	−0.606	−0.284	−0.115	−0.0344	0.000 64
	150	0.789	−1.365	−0.774	−0.420	−0.214	−0.986	−0.0374
	200	0.690	−1.474	−0.884	−0.519	−0.294	−0.158	−0.778
	250	0.631	−1.543	−0.960	−0.593	−0.359	−0.209	−0.116
	300	0.596	1.552	−1.015	−0.651	−0.412	−0.254	−0.151

[a]Numbers in parentheses denote reference from which the measured phase shift was taken.

ACKNOWLEDGMENTS

We thank Dr. D. Andrick, Dr. A. K. Bhatia, Dr. D. Filipović, Dr. W. E. Kauppila, Dr. A. D. Stauffer, and Dr. T. S. Stein for providing unpublished data. Support of the National Science Foundation (Grant No. PHY 83-11705) and the Air Force Office of Scientific Research (Grant No. AFOSR-84-0143) is gratefully acknowledged.

APPENDIX A: GENERATION OF SPHERICAL BESSEL FUNCTIONS

The standard recursion relations[76] can be used for the generation of the spherical Bessel functions $n_l(x)$ and $k_l(x)$ for any value of the argument x and for increasing l as well as for the generation of $j_l(x)$ for increasing l and for argument $x > 50$. However, due to a numerical instability, these recurrence relations cannot be used for the generation of $j_l(x)$ for increasing l if $x \lesssim 50$ and for the generation of $i_l(x)$ for increasing l for any value of the argument x. In these cases $i_l(x)$ and $j_l(x)$ can be evaluated using hypergeometric function ${}_0F_1$:

$$i_l(x)=\sqrt{\pi/2x}\,(x/2)^{l+1/2}{}_0F_1(l+\tfrac{3}{2};x^2/4)/\Gamma(l+\tfrac{3}{2})\,, \tag{A1}$$

$$j_l(x)=\sqrt{\pi/2x}\,(x/2)^{l+1/2}{}_0F_1(l+\tfrac{3}{2};-x^2/4)/\Gamma(l+\tfrac{3}{2})\,. \tag{A2}$$

The function ${}_0F_1$ can be evaluated using the rational approximation.[77] When the argument x of j_l is large (>50), the rational approximation for ${}_0F_1$ becomes unstable.

APPENDIX B: DERIVATION OF PHASE SHIFT FOR POLARIZATION POTENTIAL IN BORN APPROXIMATION

For the polarization potential, Eq. (18), the Born phase-shift integral T_{Bl}, Eq. (5), is defined to be T_{pBl} and is given by

$$T_{pBl}=\alpha k\int_0^\infty r^4 j_l^2(kr)/(r^2+d^2)^3 dr\ . \tag{B1}$$

After some simplifications, Eq. (B1) can be written as

$$T_{pBl}=\alpha k^2\left[\int_0^\infty x^2 j_l^2(x)/(x^2+a^2)^2 dx - a^2\int_0^\infty x^2 j_l^2(x)/(x^2+a^2)^3 dx\right], \tag{B2}$$

where $a=kd$. Using Eq. (6.535) of Ref. 78 and the recurrence relations for the spherical Bessel functions $i_l(x)$ and $k_l(x)$ one can derive

$$\int_0^\infty x^2 j_l^2(x)/(x^2+a^2)^2 dx = -[2a i_{l+1}(a)k_l(a)-\pi/(2a)+(2l+1)i_l(a)k_l(a)]/2(a)\ , \tag{B3}$$

$$\begin{aligned}\int_0^\infty x^2 j_l^2(x)/(x^2+a^2)^3 dx = &-[2a i_{l+1}(a)k_l(a)-\pi/(2a)+(2l+1)i_l(a)k_l(a)]/(8a^3)\\ &+\{4l i_{l+1}(a)k_l(a)-\pi l/a^2+i_l(a)k_l(a)/a\,[2a^2+4(l+\tfrac{1}{2})^2-2l-1]\\ &-2a i_{l+1}(a)k_{l+1}(a)\}/(8a^2)\ .\end{aligned} \tag{B4}$$

Substituting (B3) and (B4) in (B2) and after some simplification Eq. (20) is obtained.

APPENDIX C: DERIVATION OF PHASE SHIFT FOR STATIC POTENTIAL IN BORN APPROXIMATION

Substituting $V_s(r)$ [Eq. (17)], in Eq. (5) and making use of the standard integral[78]

$$\int_0^\infty r\exp(-zr)j_l^2(kr)dr=(2k^2)^{-1}Q_l[1+z^2/(2k^2)]\ , \tag{C1}$$

where Q_l is the Legendre function of the second kind, Eq. (22) is obtained. The argument of the Q_l function, $1+z^2/(2k^2)$, is greater than 1 and therefore the recurrence relation cannot be used for the generation of the functions for increasing l. One convenient way to evaluate a Q_l function is to write it in terms of Gaussian hypergeometric function $F(a,b;c;x)$ as[76]

$$Q_l(x)=\frac{\pi^{1/2}\Gamma(l+1)}{2^{l+1}\Gamma(l+\frac{3}{2})}\frac{1}{x^{l+1}}F(1+l/2,\tfrac{1}{2}+l/2;l+\tfrac{3}{2};1/x^2),\quad x>1 \tag{C2}$$

where the hypergeometric function can be evaluated by summing the following series:

$$F(a,b;c;x)=1+\frac{ab}{c\times 1}x+\frac{a(a+1)b(b+1)}{c(c+1)\times 1\times 2}x^2+\frac{a(a+1)(a+2)b(b+1)(b+2)}{c(c+1)(c+2)\times 1\times 2\times 3}x^3+\cdots\ . \tag{C3}$$

The higher-order derivatives of Q_l with respect to z can be carried out easily using Eq. (C2) and the relation

$$\frac{d^n}{dx^n}F(a,b;c;x)=\frac{\Gamma(a+n)\Gamma(b+n)\Gamma(c)}{\Gamma(c+n)\Gamma(a)\Gamma(b)}F(a+n,b+n;c+n;x)\ . \tag{C4}$$

[1] C. Ramsauer, Ann. Phys. (Leipzig) 66, 546 (1921).

[2] W. E. Kauppila and T. S. Stein, Can. J. Phys. 60, 471 (1982); T. S. Stein and W. E. Kauppila, Adv. At. Mol. Phys. 18, 53 (1982).

[3] G. M. A. Hyder, M. S. Dababneh, Y.-F. Hsieh, W. E. Kauppila, C. K. Kwan, M. Mahdavi-Hezaveh, and T. S. Stein, Phys. Rev. Lett. 57, 2252 (1986).

[4] G. M. Webb, Phys. Rev. 47, 379 (1935).

[5] W. Aberth, G. Sunshine, and B. Bederson, *Abstracts of the Third International Conference on the Physics of Electronic and Atomic Collisions, London, 1963,* edited by M. R. C. McDowell (North-Holland, Amsterdam, 1964), p. 53.

[6] D. E. Golden and H. W. Bandel, Phys. Rev. 149, 58 (1966).

[7] W. E. Kauppila, T. S. Stein, G. Jesion, M. S. Dababneh, and V. Pol, Rev. Sci. Instrum. 48, 822 (1977).

[8] R. W. Wagenaar and F. J. de Heer, J. Phys. B 13, 3855 (1980).

[9] R. W. Wagenaar and F. J. de Heer, J. Phys. B 18, 2021 (1985).

[10] W. E. Kauppila, T. S. Stein, J. H. Smart, M. S. Dababneh, Y. K. Ho, J. P. Downing, and V. Pol, Phys. Rev. A 24, 725 (1981).

[11] J. C. Nickel, I. Imre, D. F. Register, and S. Trajmar, J. Phys. B 18, 125 (1985).

[12] K. Jost, P. G. F. Bisling, F. Eschen, M. Felsmann, and L. Walther, in *Abstracts of Contributed Papers, Thirteenth Inter-*

national Conference on the Physics of Electronic and Atomic Collisions, Berlin, 1983, edited by J. Eichler, W. Fritsch, I. V. Hertel, N. Stolterfoht, and W. Willie (North-Holland, Amsterdam, 1983), p. 91; A. K. Bhatia (private communication).
[13]J. Ferch, B. Granitza, C. Masche, and W. Raith, J. Phys. B **18**, 967 (1985).
[14]M. Charlton, T. C. Griffith, G. R. Heyland, and T. R. Twomey, J. Phys. B **13**, L239 (1980).
[15]Yu. K. Gus'kov, R. V. Savvov, and V. A. Slobodyanyuk, Zh. Tekh. Fiz. **48**, 277 (1978) [Sov. Phys.—Tech. Phys. **23**, 167 (1978)].
[16]J. Mehr, Z. Phys. **198**, 345 (1967).
[17]K. Schackert, Z. Phys. **213**, 316 (1968).
[18]J. P. Bromberg, J. Chem. Phys. **61**, 963 (1974).
[19]J. F. Williams and B. A. Willis, J. Phys. B **8**, 1670 (1975).
[20]R. H. J. Jansen, F. J. de Heer, H. J. Luyken, B. van Wingerden, and H. J. Blaauw, J. Phys. B **9**, 185 (1976).
[21]B. R. Lewis, J. B. Furness, P. J. O. Teubner, and E. Weigold, J. Phys. B **7**, 1083 (1974).
[22]L. Vušković and M. V. Kurepa, J. Phys. B **9**, 837 (1976).
[23]R. D. DuBois and M. E. Rudd, J. Phys. B **9**, 2657 (1976).
[24]S. C. Gupta, Ph.D. thesis, University of Liverpool, 1975 (the data are quoted in Ref. 31).
[25]S. C. Gupta and J. A. Rees, J. Phys. B **8**, 1267 (1975).
[26]J. F. Williams, J. Phys. B **12**, 265 (1979).
[27]S. K. Srivastava, H. Tanaka, A. Chutjian, and S. Trajmar, Phys. Rev. A **23**, 2156 (1981).
[28]D. Andrick (private communication).
[29]Zhou Qing, M. J. M. Beerlage, and M. J. van der Weil, Physica C **113**, 225 (1982).
[30]Dusan M. Filipović, M. Sci. thesis, Institute of Physics, Beograd, 1984.
[31]F. J. de Heer, R. H. J. Jansen, and W. van der Kaay, J. Phys. B **12**, 979 (1979).
[32]D. A. McPherson, R. K. Feeney, and J. W. Hooper, Phys. Rev. A **13**, 167 (1976).
[33]K. S. Golovanivsky and A. P. Kabilan, Phys. Lett. **80A**, 249 (1980).
[34]G. N. Haddad and T. F. O'Malley, Aust. J. Phys. **35**, 35 (1982).
[35]D. W. Walker, Adv. Phys. **20**, 257 (1971).
[36]M. Fink and A. C. Yates, At. Data **1**, 385 (1970).
[37]D. G. Thompson, Proc. R. Soc. London, Ser. A **294**, 160 (1966); J. Phys. B **4**, 468 (1971).
[38]A. Garbaty and R. W. LaBahn, Phys. Rev. A **4**, 1425 (1971).
[39]A. W. Yau, R. P. McEachran, and A. D. Stauffer, J. Phys. B **11**, 2907 (1978).
[40]A. Dasgupta and A. K. Bhatia, Phys. Rev. A **32**, 3335 (1985).
[41]W. C. Fon, K. A. Berrington, P. G. Burke, and A. Hibbert, J. Phys. B **16**, 307 (1983).
[42]K. L. Bell, N. S. Scott, and M. A. Lennon, J. Phys. B **17**, 4757 (1984).
[43]M. S. Pindzola and H. P. Kelly, Phys. Rev. A **9**, 323 (1974).
[44]M. Ya. Amusia, N. A. Cherepkov, L. V. Chernysheva, D. M. Davidović, and V. Radojević, Phys. Rev. A **25**, 219 (1982).
[45]I. E. McCarthy, C. J. Noble, B. A. Phillips, and A. D. Turnbull, Phys. Rev. A **15**, 2173 (1977).
[46]C. J. Joachain, R. Vanderpoorten, K. H. Winters, and F. W. Byron, Jr., J. Phys. B **10**, 227 (1977).
[47]C. J. Joachain, *Proceedings of the Tenth International Conference on the Physics of Electronic and Atomic Collisions, Paris, 1977,* edited by G. Watel (North-Holland, Amsterdam, 1977), p. 71.
[48]G. Staszewska, D. W. Schwenke, and D. G. Truhlar, Phys. Rev. A **29**, 3078 (1984).
[49]R. A. Berg, J. E. Purcell, and A. E. S. Green, Phys. Rev. A **3**, 508 (1971).
[50]S. K. Datta, S. K. Mandal, P. Khan, and A. S. Ghosh, in *Proceedings of the Seventh International Conference on Positron Annihilation (ICPA),* edited by P. C. Jain, R. M. Singru, and K. P. Gopinathan (World Scientific, Singapore, 1985), p. 387; Phys. Rev. A **32**, 633 (1985).
[51]S. P. Khare and P. Shobha, J. Phys. B **7**, 420 (1974).
[52]R. P. McEachran and A. D. Stauffer, J. Phys. B **16**, 4023 (1983).
[53]R. Haberland, L. Fritsche, and J. Noffke, Phys. Rev. A **33**, 2305 (1986).
[54]L. S. Frost and A. V. Phelps, Phys. Rev. **136**, A1538 (1964).
[55]H. B. Milloy, R. W. Crompton, J. A. Rees, and A. G. Robertson, Aust. J. Phys. **30**, 61 (1977).
[56]K. F. Canter, P. G. Coleman, T. C. Griffith, and G. R. Heyland, Appl. Phys. **3**, 249 (1974).
[57]B. Jaduszliwer and D. A. Paul, Can. J. Phys. **52**, 272 (1974); T. S. Stein (private communication).
[58]W. E. Kauppila, T. S. Stein, and G. Jesion, Phys. Rev. Lett. **36**, 580 (1976).
[59]P. G. Coleman, T. C. Griffith, G. R. Heyland, and T. R. Twomey, Appl. Phys. **11**, 321 (1976).
[60]T. C. Griffith, G. R. Heyland, and T. R. Twomey, as reported by T. C. Griffith and G. R. Heyland, Phys. Rep. **39**, 169 (1978).
[61]J-S. Tsai, L. Lebow, and D. A. L. Paul, Can. J. Phys. **54**, 1741 (1976).
[62]A. G. Brenton, J. Dutton, and F. M. Harris, J. Phys. B **11**, L15 (1978).
[63]G. Sinapius, W. Raith, and W. G. Wilson, J. Phys. B **13**, 4079 (1980).
[64]P. G. Coleman, J. D. McNutt, L. M. Diana, and J. T. Hutton, Phys. Rev. A **22**, 2290 (1980); T. S. Stein (private communication).
[65]T. S. Stein and W. E. Kauppila, in *Proceedings of the Fourteenth International Conference on the Physics of Electronic and Atomic Collisions,* edited by D. C. Lorents, W. E. Meyerhof, and J. R. Peterson (North-Holland, Amsterdam, 1986), p. 105.
[66]P. G. Coleman and J. D. McNutt, Phys. Rev. Lett. **42**, 1130 (1979).
[67]S. P. Khare, A. Kumar, and K. Lata, Indian J. Pure Appl. Phys. **20**, 379 (1982); Phys. Rev. A **33**, 2795 (1986).
[68]R. P. McEachran, A. G. Ryman, and A. D. Stauffer, J. Phys. B **12**, 1031 (1979).
[69]R. P. McEachran and A. D. Stauffer, in *Proceedings of the Third International Workshop on Positron (Electron)-Gas Scattering,* edited by W. E. Kauppila, T. S. Stein, and J. M. Wadehra (World Scientific, Singapore, 1986), p. 122.
[70]P. U. Arifov and G. I. Zhuravleva, in *Proceedings of the Seventh International Conference on Positron Annihilation (ICPA),* edited by P. C. Jain, R. M. Singru, and K. P. Gopinathan (World Scientific, Singapore, 1985), p. 425.
[71]E. Clementi and C. Roetti, At. Data Nucl. Data Tables **14**, 177 (1974).
[72]B. L. Jhanwar and S. P. Khare, Phys. Lett. **50A**, 201 (1974).
[73]M. E. Riley and D. G. Truhlar, J. Chem. Phys. **63**, 2182 (1975); J. B. Furness and I. E. McCarthy, J. Phys. B **6**, 2280 (1973); B. H. Bransden, M. R. C. McDowell, C. J. Noble, and T. Scott, *ibid.* **9**, 1301 (1976).
[74]See, for example, E. W. McDaniel and E. A. Mason, *The Mobility and Diffusion of Ions in Gases* (Wiley, New York, 1973).

[75]J. M. Wadehra, T. S. Stein, and W. E. Kauppila, Phys. Rev. A 29, 2912 (1984).

[76]See, for example, *Handbook of Mathematical Functions*, edited by M. Abramowitz and I. A. Stegun (Dover, New York, 1970).

[77]See, for example, Yudell L. Luke, *Algorithms for the Computation of Mathematical Functions* (Academic, New York, 1977).

[78]See, for example, *Table of Integrals, Series, and Products*, edited by I. S. Gradshteyn and I. M. Ryzhik (Academic, New York, 1980).